Journal of Applied Polymer Science

Cellulose Nanofibers Prepared from TEMPO-oxidation of Kraft Pulp and Its Flocculation Effect on Kaolin Clay

Liqiang Jin,[1] Yanwei Wei,[1] Qinghua Xu,[2] Wenrun Yao,[2] Zhengliang Cheng[2]

[1]Department of Applied Chemistry, School of Chemistry and Pharmaceutical Engineering, Qilu University of Technology, Jinan 250353, China

[2]Key Laboratory of Paper Science and Technology of Ministry of Education, Department of Pulp and Paper Engineering, Qilu University of Technology, Jinan 250353, China

Correspondence to: L. Jin (E-mail: jlq@qlu.edu.cn)

ABSTRACT: Cellulose nanofibers were prepared using TEMPO/NaBr/NaClO oxidation of kraft pulp and successive ultrasonic treatment, and the properties were characterized by conductimetric titration, X-ray diffraction, and atomic force microscopy. The resulting product was then applied as an anionic microparticle to constitute a microparticulate system with cationic polyacrylamide (CPAM), to induce the flocculation of the kaolin clay suspension. The flocculation effect was evaluated by determining the relative turbidity of clay suspension. The results showed that the obtained cellulose nanofibers had cellulose I structure with higher crystallinity than that of the kraft pulp, and their cross-sectional dimension was in the range of 3–5 nm. They had more negative zeta potential at neutral and alkaline conditions. It was found that the microparticulate system showed high flocculation effect on kaolin clay at a very low level of nanofiber addition, and a high shear level after CPAM addition was helpful for the flocculation. © 2014 Wiley Periodicals, Inc. J. Appl. Polym. Sci. **2014**, *131*, 40450.

KEYWORDS: cellulose and other wood products; applications; clay; fibers; crystallization

Received 28 November 2013; accepted 14 January 2014

DOI: 10.1002/app.40450

INTRODUCTION

With increasing paper machine running speed, recycled fiber utilization and water closed circulation, increased retention of fine fibers and fillers and improvement of the runnability of the paper machine are becoming more important in the paper industry.[1–3] Therefore, the demands on retention and drainage aids are greatly increasing. Fillers place particularly high demands on retention aids. Not only because filler particles are too small to be directly retained by the typical forming fabrics used on paper machines, but also because the specific surface area is relatively high.[4] The mechanism for filler and fines retention depends on mechanical entrapment and colloidal aggregation. In modern high-speed paper machines, such as twin-wire gap formers, the mechanical entrapment for filler retention is significantly reduced, and consequently the importance of colloidal aggregation increases.[5] However, conventional retention aids, such as natural and synthetic polymers,[6] are not effective on high-speed paper machines, where high-shear forces tend to disrupt formed flocs.[7] Microparticle retention and drainage aid system is widely used in high-speed paper machines, which not only increases the fines and fillers retention and improves the pulp drainage but also provides produced papers with a better formation and air permeability.[8] Much of the literature on microparticle applications in the papermaking industry pertains to anionic microparticles used in conjunction with a cationic polymer of high molecular weight.[9–11] In the first stage of this retention system, the cationic polyelectrolyte (cationic polyacrylamide or cationic starch) adsorbs onto fibers, fines, and fillers resulting in aggregates which are dispersed in areas with high shear rates. Then, an anionic microparticle (bentonite or colloidal silica) is added to the suspension to form bridges between polymer layers on the surfaces of paper components and to reflocculate the system.[11,12] Surface charge of fibers, conformational behavior of the cationic polymer on the surfaces, and the number of extended parts (loops and tails) of the cationic polymer affect the adsorption of anionic microparticles (bentonite or colloidal silica).[13] The shape and size of microparticles play key roles in the retention improvement and drainage promotion. An increase in flocculation effectiveness or first-pass retention is consistent with the increase in particle size of microparticles.[14] Montmorillonite has a high bridging ability due to its high width to thickness ratio. Mueller et al. found that the microparticle had a dominant effect on flocculation whenever bentonite was used.[15]

Cellulose is the most abundant renewable biopolymer which presents primarily in wood biomass.[16] For the past few decades, cellulose has attracted attention as one of the promising polysaccharides for accomplishing highly engineered nanoparticles, which can be applied in many areas.[17–20] By applying mechanical, chemical, physical, or biological methods, cellulosic fibers can be disintegrated into cellulose substructures with microsize or nanosize dimensions.[21] Nanocellulose demonstrates excellent properties, including high aspect ratio, large specific surface area, unique optical properties, and high Young's modulus resulting from high crystallinity.[22] Furthermore, it has the advantages of bio-based materials such as being light-weight, biodegradable, biocompatible, and renewable.[23]

Turbak et al. discovered nano fibrillation cellulose (NFC) and first suggested their application in papers in 1983.[24] It was reported that NFC can be used for improving the physical properties of papers and cellulosic films.[25–27] Cellulose nanofibrils prepared by 2,2,6,6-tetramethyl-piperidine-1-oxyl (TEMPO)-mediated oxidation of native cellulose followed by mechanical disintegration, namely TOCN, have uniform widths of 3–4 nm and lengths of a few microns.[28] When TEMPO/NaBr/NaClO oxidation is applied to native celluloses, the C6 primary hydroxyls of cellulose can be entirely and selectively converted to sodium carboxylate groups.[29] The high aspect ratio, nanometer width, and the high negative charge nature may impart TOCN a high bridging ability, thus constituting a microparticulate system with a cationic polymer that retains the fillers by inducing flocculation among filler particles. In our previous study,[30] nanocrystalline cellulose (NCC) was prepared from bleached aspen kraft pulp through sulfuric acid hydrolysis and then applied as pulp strengthening additive and retention aid in the deinked pulp. The formation of microparticulate retention systems during the application of NCC together with cationic polyacrylamide and cationic starch was able to improve pulp retention and strength properties without negative influence on drainage.

The aim of this study was to investigate the effect of nanocellulose on the flocculation of kaolin clay, a widely used filler in a variety of paper grades. TOCN, prepared by using TEMPO/NaBr/NaClO oxidation of kraft pulp combined with ultrasound treatment, was applied in the kaolin clay suspension, as an anionic microparticle to constitute a microparticulate system with cationic polyacrylamide (CPAM), to induce the flocculation between clay particles. It was found that the CPAM/TOCN system showed high flocculation effect at a very low level of TOCN addition. A high shear level after CPAM addition was helpful for the flocculation.

EXPERIMENTAL

Materials

Bleached softwood kraft pulp was provided by Yinxing Paper (Jinan, China). The 2,2,6,6-tetramethyl-piperidine-1-oxyl (TEMPO) with purity of 99% was purchased from Sigma–Aldrich. Cationic polyacrylamide (CPAM) with molecular weight of 5–8 million and a charge density of 1114.28 μeq g^{-1} was provided by Huatai Group (Dongying, China). Kaolin clay was purchased from Sinopharm Chemical Reagent, with average particle size of 6.5 μm. The other chemicals used were all analytical pure reagents.

TEMPO/NaBr/NaClO-oxidation

TEMPO/NaBr/NaClO-oxidation was carried out in a three-neck round bottom flask. About 1 g of never-dried pulp in 100 mL water was added to the flask, and the pulp suspension was stirred continuously at 400–500 rpm with an overhead stirrer. NaBr (0.1 g, 0.97 mmol) and TEMPO (0.016 g, 0.1 mmol) were added to the pulp suspension, and then a certain amount of NaClO, corresponding to 2, 4, 6, 8, 10 mmol g^{-1} pulp, was slowly added into the solution. The pH of the mixture was maintained at 10.0–10.5 by the addition of a Na_2CO_3-$NaHCO_3$ buffer solution. The reaction was carried out at 25°C for 24 h, and then was stopped by adding 100 mL of ethanol. The oxidized pulp was recovered by vacuum filtration, washed several times with deionized water to neutral pH, and then dialyzed against deionized water for 5 days. The resultants were stored as a never-dried state at 5°C. The carboxyl content of each sample was determined by conductometric titration as described below.

Preparation of Cellulose Nanofibers

The above TEMPO-oxidized pulps were sonicated to obtain cellulose nanofibers. The sonication was performed with a Bilon-500 Ultrasonic Sonifier for 20 min (with power of 300 *W*, each circulation with 1 s of ultrasonic wave, and 8 s of interval), in a specially designed double-walled beaker connected to a cooling bath to minimize overheating of suspensions. After ultrasonication, a small amount of residue unfibrillated fibers, floating in the sonicated suspensions, were removed by centrifugation (4500 rpm, 30 min) using a centrifuge. The acquired dispersions, namely TOCN1-TOCN5, according to the NaClO addition of 2–10 mmol g^{-1} pulp, were stored at 5°C until used.

Characterization of TOCN

Zeta potential of TOCNs at various pH was measured with a Malvin Zetasizer. The carboxylate content of the oxidized pulp was determined by conductimetric titration with a DDS-11A Digital Conductivity Meter (Shanghai Hongyi Instrumentation, China). Nearly 50 mg of cellulose sample was suspended into 15 mL of 0.01 M hydrochloric acid solution. After being stirred for 10 min, the suspensions were titrated with 0.01 M NaOH standard solution. The titration curve was obtained and the total amount of carboxyl groups was calculated based on the following equation,

$$C = \frac{(V_1 - V_0) \times C_{NaOH}}{m}$$

where C is the carboxyl content; V_1 and V_0, are the equivalent volumes of added NaOH solution; C_{NaOH}, is the concentration of NaOH solution, and m is the dry weight of oxidized fiber.

X-ray diffraction analysis was performed with a D8 Powder X-ray diffractometer (Bruker AXS, Germany), which was equipped with a Cu Kα X-ray tube. The crystallinity was calculated according to the X-ray diffraction curve by the ratio of the crystalline area to the total area.[31]

A Multimode 8 Nanoscope V System AFM (Bruker Corporation, Germany) was used for studying the surface characteristics of the NCC samples. A drop of sample was air dried overnight

Table I. Effect of NaClO Addition on the Carboxyl Content, Zeta Potential, DP, Yield, and Crystallinity of Aspen Kraft Pulp and TOCNs

Sample	Carboxyl content (mmol g^{-1})	Zeta potential (mv)	Yield (%)	DP	Crystallinity (%)
Bleached kraft pulp	0.02	−21.2	-	1200	56.8
TOCN1	1.17	−33.6	99.0	480	67.7
TOCN2	1.59	−42.0	98.0	430	72.3
TOCN3	1.87	−57.1	97.0	350	77.3
TOCN4	2.0	−63.5	95.0	320	81.7
TOCN5	2.03	−67.8	94.8	310	80.9

on a clean mica surface at ambient conditions for the analysis. Images from several different places on the samples were scanned.

DP values of TOCNs were measured according to the literature.[32] About 0.5 g of TOCN samples were further treated with 50 mL of 1% $NaClO_2$ at pH 4.8 and room temperature for 2 days to oxidize small amounts of C6-aldehydes present in the oxidized cellulose to carboxyls. All carboxyl groups were converted to sodium carboxylate groups with a diluted NaOH solution. The $NaClO_2$-oxidized TOCNs were then dialyzed against water and subsequent freeze dried. The intrinsic viscosity measurements were performed according to ISO 5351-1(1981, option B) with cupriethylendiamine as the solvent. Degree of polymerization was calculated from intrinsic viscosity data.

Flocculation

The flocculation experiment was carried out according to the literature[33] by using a photometric dispersion analyzer (PDA2000, Rank Brothers, UK), which was connected to a dynamic drainage jar (DDJ). The degree of flocculation was evaluated by the relative turbidity, calculated from the variation of direct current voltage signals. First, 500 mL of tap water was poured into a DDJ without mesh and circulated for several minutes to keep the flow steady. Then, 8 mL of clay suspension (100 mg L^{-1}) was added to the DDJ at a rotation speed of 500 rpm. The clay in the DDJ was circulated through the PDA in a plastic tube at a flow rate of 20 mL min^{-1}. The initial base voltage (V_0) was reduced to the unflocculated suspension voltage (V_i). After 200 s, the rotation speed was increased to 750 rpm, and CPAM was added to induce the flocculation of clay. Nearly 30 s later, the rotation speed was further increased to 1500 rpm and maintained for 30 s. Then, the rotation speed was lowered to 500 rpm and a certain amount of TOCN was added to reflocculate the clay. The final suspension voltage (V_f) was recorded 90 s after the TOCN addition. The relative turbidity was calculated according to the equation below,

$$Relative\ turbidity = \frac{\ln V_0/V_f}{\ln V_0/V_i}$$

where V_o is the initial base DC voltage, V_i is the unflocculated suspension DC voltage, and V_f is the final suspension voltage.

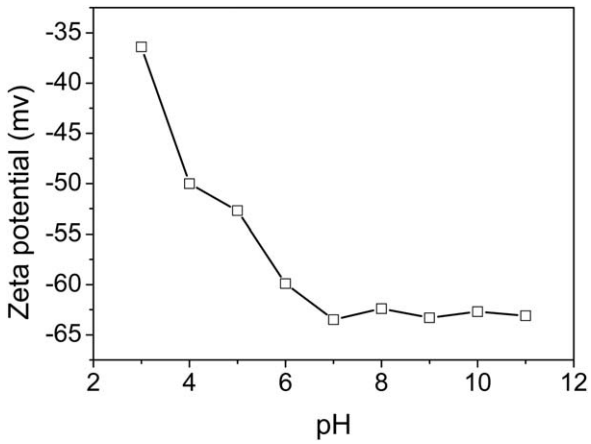

Figure 1. Zeta potential of TOCN 4 at various pH.

RESULTS AND DISCUSSION

Characterization of TOCNs

Table I shows the carboxyl content, crystallinity, DP and yield of aspen kraft pulp and TOCNs. The carboxylate content increased significantly after the oxidation, which suggested the formation of anionic carboxylate groups with high density on the nanofiber surface. This is in agreement with the results of the prior literatures.[28,34] The carboxylate content increased with the increase of added NaClO, and it reached a plateau when NaClO addition was 8 mmol g^{-1}.

The negative zeta potential of TOCNs increased with the increase of the NaClO addition, which is consistent with the increase of the carboxylate content. Zeta potential of TOCN4

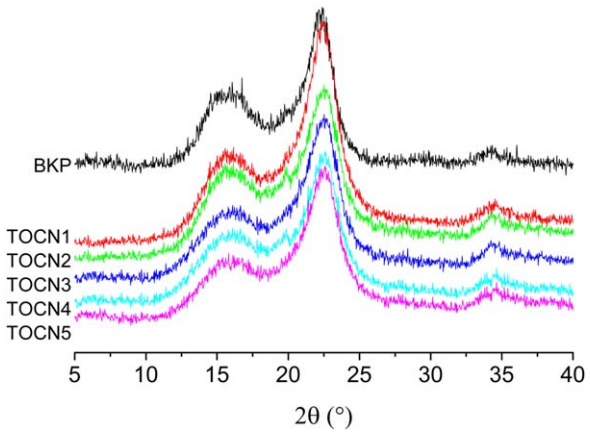

Figure 2. Wide-angle X-ray diffraction patterns of kraft pulp and TOCNs. [Color figure can be viewed in the online issue, which is available at wileyonlinelibrary.com.]

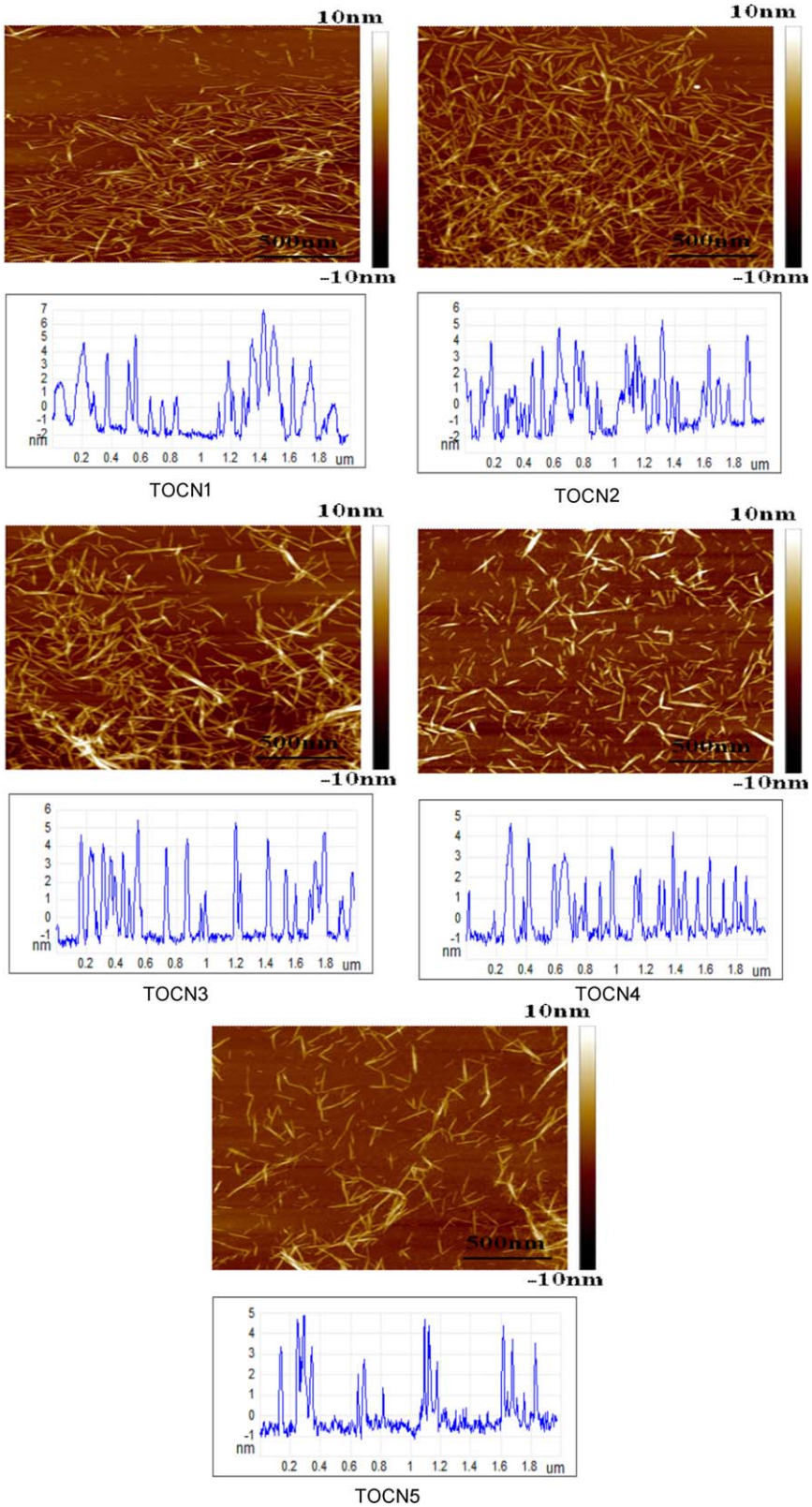

Figure 3. Dimensional dynamic AFM image of TOCN. Z-profile graphs were taken across the image from an arbitrary horizontal line. [Color figure can be viewed in the online issue, which is available at wileyonlinelibrary.com.]

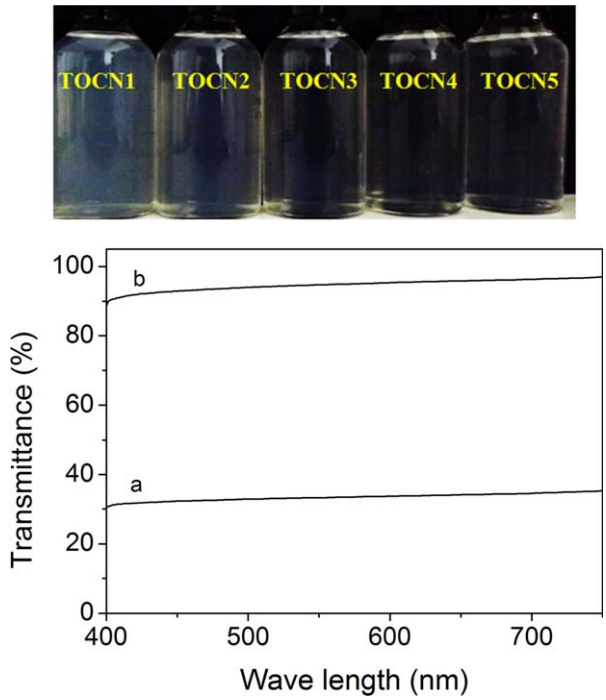

Figure 4. Dispersion states and visible light transmittance of TOCN1(a) and TOCN4 (b). [Color figure can be viewed in the online issue, which is available at wileyonlinelibrary.com.]

versus pH is shown in Figure 1. Obviously, it was significantly affected by the pH of the solution. Zeta potential was more negative with the increase of pH from 3 to 6, and remained unchanged under neutral and moderately alkaline conditions, due to the dissociation of carboxylate groups. This attribute is very important to extend its application in the papermaking process, because the environment of the wet end of papermaking is usually under neutral or mild alkaline conditions.

Carboxylate content is the key factor that influences the degree of nanofiber conversion of TEMPO-oxidized celluloses.[35] The yields of TOCNs were more than 90%, which was in accordant with the results of Saito et al.,[36] who proved that TEMPO-mediated oxidation facilitated the defibrillation process. Besbes et al.[37] reported that when the carboxylate content was more than 0.5 mmol g^{-1}, the nanofiber yields exceeded 90%.

As shown in Table I, DP values of TOCNs were far lower than that of the kraft pulp (1200), indicating a significant depolymerization during the TEMPO-oxidation. This is consistent with the results of Fukuzumi,[38] who reported a DP value decrease from 1200 to ~250–400 by TEMPO-oxidation with 5–10 mmol g^{-1} of NaClO.

The wide-angle X-ray diffraction patterns of kraft pulp and TOCNs were investigated (Figure 2). The peaks at $2\theta = 14–18°$, 22.5°, and 34.5°, which were characteristic of the structure of cellulose I,[39] indicated that the crystal structure of cellulose I was not changed after the oxidation. Compared to the untreated kraft pulp, higher crystallinity was achieved for the TOCNs.

The cellulose nanofibers were observed using an atomic force microscope, and their morphologies are shown in Figure 3. The nanofibers were rod-like crystals, with cross-sections in nanometer range. Their morphology were quite similar to what has been reported in the literature.[40] The height profiles of the line along the length of the cellulose nanofibers were plotted, which revealed that the widths of the nanofibers were in the range of 3–5 nm. The widths changed insignificantly irrespective of the amount of NaClO used during the oxidation process. However, the lengths decreased with the increase of the NaClO addition, which agrees well with the results reported before.[28] The dispersibility of TOCN by using a larger amount of NaClO was better, likely due to the higher carboxylate content introduced during the oxidation, which consequently increased electrostatic repulsions between the nano particles. The appearance of TOCN dispersions varied from translucent to transparent (Figure 4).With the increase of the NaClO addition, the transparency was improved. The low transparency of TOCN1 might result from the aggregates of nanocellulose fibers (Figure 3). In contrast, individual nanofibers with widths of 3–5 nm were obtained with a higher amount of NaClO addition, due to the formation of more carboxylate contents. The widths were smaller than the wave length of visible light, which caused the high transparency of the dispersions.[28] The light transmittance rate of TOCN1 and TOCN4 was measured as examples of low and high carboxylate contents, respectively (Figure 4). The transparency was confirmed by the transmittance curve of TOCN under visible light.

Flocculation Effect of CPAM/TOCN on Kaolin Clay

TOCN4, with a cayboxyalte content of 2.0 mmol g^{-1} and a uniform width of 3–5 nm, was used as an anionic microparticle, together with CPAM, consitituting a microparticle retention system, to investigte its flocculation effect on kaolin clay. The effect of TOCN addition on the relative turbidities is shown in Figure 5. The relative turbidity decreased from 1.0 to 0.87 by adding the negatively charged nanocellulose alone, suggesting that a weak flocculation was induced. This is very similiar to the action of anionic high molecular mass polymer reported by Liu et al.[41] Nanocellulose might be considered as a potential natural retention aid due to its large surface area and high aspect ratio.[30] Bridges between clay particles could be formed by long and

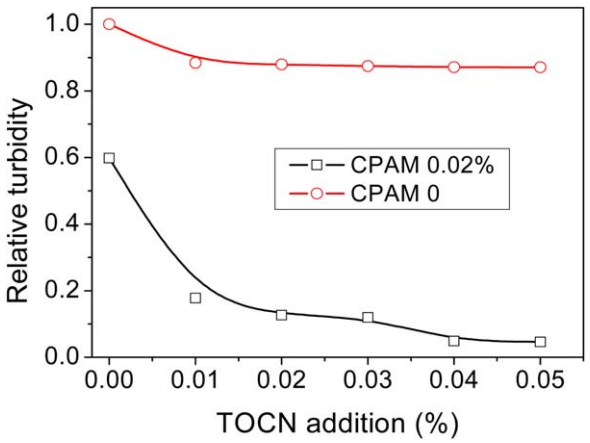

Figure 5. Effect of TOCN addition on the relative turbidity of kaolin clay suspension. [Color figure can be viewed in the online issue, which is available at wileyonlinelibrary.com.]

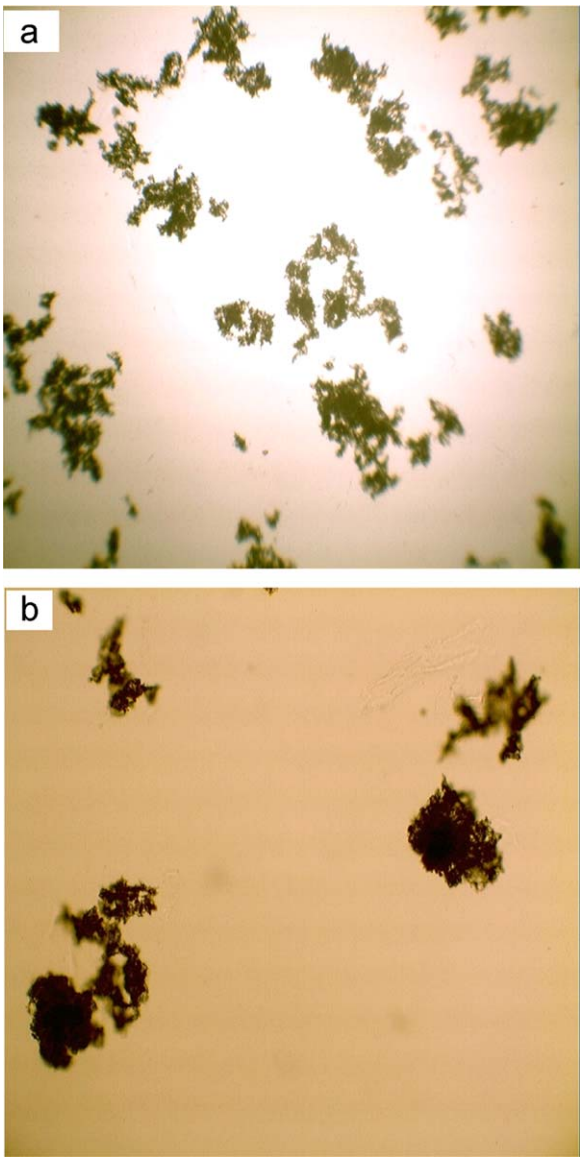

Figure 6. Optical micrographs of kaolin clay flocs without(a) and with(b) adding TOCN. [Color figure can be viewed in the online issue, which is available at wileyonlinelibrary.com.]

narrow nanofibers, thus inducing the weak flocculation. When CPAM was added to constitute a microparticulate retention system with TOCN, the turbidity greatly decreased, indicating an improved flocculation. The addition of CPAM resulted in the primary flocculation of kaolin clay, which is shown in Figure 6(a). These flocs were large, loose and easily broken down by shear forces mainly through breakage of polymer chains.[4] The redistribution of CPAM may create fresh CPAM-covered surfaces, which refers to surfaces covered with CPAM with extended conformation. Then, nanocellulose whiskers interacted with the CPAM chains with loops and tails to form folcs between clay particles, and thus induced a rapid consolidation and dewatering of the floc, resulting in smaller, denser, and stronger flocs, as shown in Figure 6(b). The relative turbidities decreased with the increase of TOCN addition and reached the minimum at an addition of 0.04%, much fewer than the dosage of conventional microparticles, which suggests that the bridging effect of nanocellulose among the CPAM-covered clay particles played an important role in the flocculation.

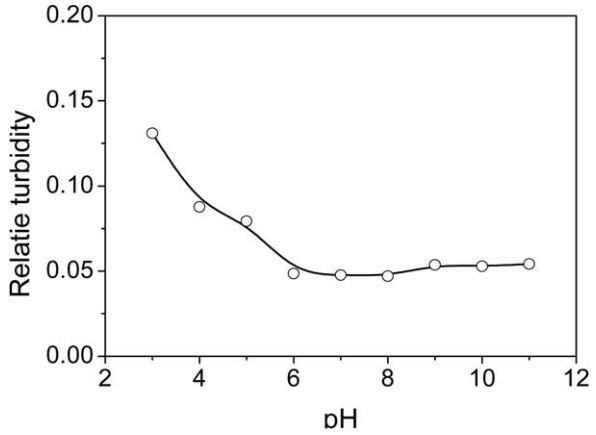

Figure 7. Effect of pH on the relative turbidity of kaolin clay suspension.

Effect of pH on the Clay Flocculation

The influence of pH on the clay flocculation is shown in Figure 7. The CPAM and TOCN addition were 0.02 and 0.04%, respectively. The relative turbidity decreased when the pH varied from pH 3–6 and reached a plateau when the pH was higher. The maximum flocculation was obtained under neutral or mild alkaline conditions, which is consistent with the change of zeta potential of nanocellulose at various pH (Figure 2). pH influences the zeta potential of nanocellulose and kaolin clay, and hence may affect the CPAM adsorption on the clay particles, as well as the interaction between clay-adsorbed CPAM and nanocellulose. The more negative zeta potential of nanocellulose, the lower relative turbidity of kaolin clay suspension. The decrease in turbidity may be attributed to the improvement of the electrostatic attraction between nanocellulose and clay-adsorbed CPAM chains, resulting from the more negative zeta potential of nanocellulose. The relative turbidity at various pH and zeta potential did not change significantly (from about 0.15–0.05), which indicates that in this

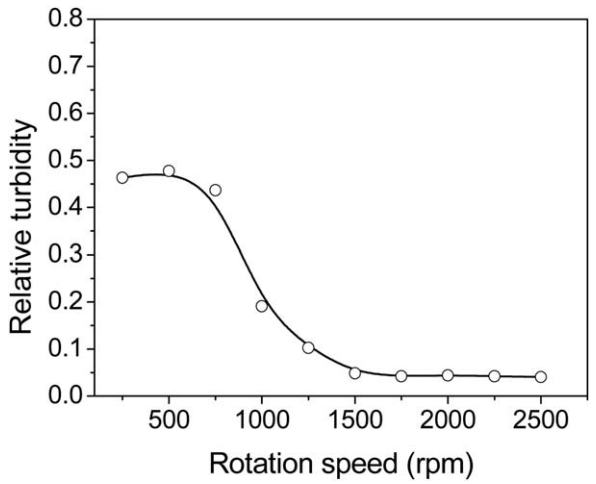

Figure 8. Effect of rotation speed after CPAM addition on the relative turbidity of clay suspension.

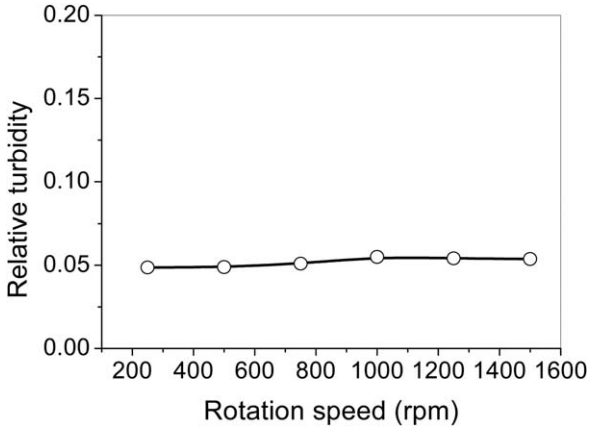

Figure 9. Effect of rotation speed after TONC addition on the relative turbidity of kaolin clay suspension.

CPAM/TOCN microparticulate system, although electrostatic and bridging effects function together to improve the flocculation of fillers, bridging effect plays a more important role at this level of TOCN addition.

Influence of Shear on the Flocculation of Kaolin Clay

Retention aid performance is affected by shear.[1] Various studies have shown that flocs formed by CPAM do not form to the same extent again after application of strong hydrodynamic shear.[4] In a typical microparicle application, the polymeric bridges formed by a cationic flocculant are partly broken as the furnish passes through a pressure screen before the addition of anionic microparticle. The influence of shear after CPAM addition on the relative turbidity of clay suspension is illustrated in Figure 8. The stirring of DDJ propeller was used to imitate the shear in the papermaking process, and the addition of CPAM and TOCN were 0.02 and 0.04%, respectively. The relative turbidity remained unchanged when the rotation speed was lower than 500 rpm, and decreased gradually with higher rotation speed. The minimum relative turbidity was obtained when the rotation speed reached 1500 rpm, and kept almost unchanged even at a rotation speed of 2500 rpm. As the literature reported,[4] the shear force can reduce the flocculant's molecular mass and break down the flocs induced by the cationic polymer before the microparticles are added. This exposes an increased number of shorter but active CPAM chains with extended conformation, which are liable to interact with the microparticles, and therefore enhance the reflocculation. A feature that sets microparticle systems apart from single or dual polymer systems is their ability to reflocculate.[42] The CPAM/TOCN system demonstrates a strong ability to reflocculate after shearing, providing strong and dense flocs.

Another feature of the microparticulate systems is the stronger shear resistance of induced flocculation. A floc's ability to resist shear and turbulence in a paper machine headbox and forming section is essential for its retention. If flocs are sensitive to these hydrodynamic forces, they will break down, pass through the forming fabrics, and accumulate in the white water.[5] The shear resistance property of clay flocculations induced by the CPAM/TONC system was investigated by determining the relative turbidity of clay suspension at varied rotation speed of DDJ after the TONC was added, as shown in Figure 9. The relative turbidity remained almost unchanged when the rotation speed was increased from 250 to 1500 rpm, indicating a high shear resistance of flocculation induced by the CPAM/TONC system, which may result from the large bridging capacity of TOCN and the strong and dense flocs formed after its addition.

CONCLUSIONS

Cellulose nanofibers were prepared by using TEMPO/NaBr/NaClO oxidation of kraft pulp and successive ultrasound treatment, and applied as an anionic microparticle to constitute a microparticulate system with CPAM to flocculate the kaolin clay suspension. The carboxylate content increased significantly after the oxidation, which gave high dispersibility for the TOCN sample. The resulting cellulose nanofibers maintained their crystalline form of cellulose I with higher crystallinity than that of the kraft pulp, and their widths were in the range of 3–5 nm. Zeta potential of TOCN was significantly affected by the pH value. It was more negative with the increase of pH from 3 to 7, and kept stable under the moderately alkaline conditions. The flocculation effect of TOCN on kaolin clay was demonstrated by the measurement of the relative turbidity of the clay suspension. The relative turbidity decreased from 1.0 to 0.87 by adding TOCN alone, suggesting that a weak flocculation was induced. When TOCN was used as an anionic microparticle to constitute a microparticulate system with CPAM, the relative turbidity decreased greatly, indicating a synergistic flocculation effect. The CPAM/TOCN system gave a higher flocculation degree under neutral and weak alkaline conditions and also at a high level of shear after the CPAM addition. The flocs induced by CPAM/TOCN were stronger and hence have higher shear resistance than those by CPAM alone.

ACKNOWLEDGMENTS

The authors would like to thank the National Natural Science Foundation of China (Grant No. 30972327, 31370581), Shandong Provincial Outstanding Youth Scholar Foundation for Scientific Research (Grant No.2009BSB01053 and BS2010CL041), and the funding of Shandong provincial Science and Technology Development Project (Grant No. 13fz02).

REFERENCES

1. Allen, L. H.; Lapointe, C. L. *Pulp Pap. Can.* **2005**, *106*, 102.
2. Main, S.; Simonson, P. *TAPPI J.* **1999**, *82*, 78.
3. Ovenden, C.; Xiao, H. N.; Wiseman, N. *TAPPI J.* **2000**, *83*, 80.
4. Hubbe, M. A.; Nanko, H.; McNeal, M. R. *BioResources* **2009**, *4*, 850.
5. Gill, R. I. S. *Pap. Technol.* **1991**, *32*, 34.
6. WÅgberg, L.; BjÖrklund, M.; Åsell, I.; Swerin, A. *TAPPI J.* **1996**, *79*, 157.
7. Yan, Z.; Deng, Y. *Chem. Eng. J.* **2000**, *80*, 31.
8. Andersson, K.; Lindgren, E. *Nord. Pulp Paper. Res. J.* **1996**, *11*, 15.

9. Honig, D. S.; Harris, E. W.; Pawlowska, L. M.; O'Toole, M. P.; Jackson, L. A. *TAPPI J.* **1993**, *76*, 135.
10. Wiputri, Y.; Englezos, P. *Recent Pat. Eng.* **2007**, *1*, 177.
11. Alince, B.; Bednar, F.; van de Ven, T. G. M. *Colloid Surf. A.* **2001**, *190*, 71.
12. Asselman, T.; Alince, B.; Garnier, G.; van de Ven, T. G. M. *Nord. Pulp Paper Res. J.* **2001**, *15*, 515.
13. Asselman, T.; Garnier, G. *Colloid Surf. A* **2000**, *174*, 297.
14. Hubbe, M. A. *TAPPI J.* **2005**, *4*, 423.
15. Mueller, P.; Gruber, E.; Schempp, W. *Wochenbl. Papierfabr.* **2001**, *129*, 36.
16. John, M. J.; Thomas, S. *Carbohydr. Polym.* **2008**, *71*, 343.
17. Fortunati, E.; Puglia, D.; Monti, M.; Santulli, C.; Maniruzzaman, M.; Kenny, J. M. *J. Appl. Polym. Sci.* **2012**, *128*, 3220.
18. Mihranyan, A.; Esmaeili, M.; Razaq, A.; Alexeichik, D.; Lindstrom, T. *J. Mater. Sci.* **2012**, *47*, 4463.
19. Eyley, S.; Thielemans, W. *Chem. Commun.* **2011**, *47*, 4177.
20. Liu, S.; Tao, D.; Bai, H.; Liu, X. *J. Appl. Polym. Sci.* **2012**, *126*, E282.
21. Fujisawa, S.; Okita, Y.; Fukuzumi, H.; Saito, T.; Isogai, A. *Carbohydr. Polym.* **2011**, *84*, 579.
22. Pei, A.; Butchosa, N.; Berglund, L. A.; Zhou, Q. *Soft Matter.* **2013**, *9*, 2047.
23. Peng, B. L.; Dhar, N.; Liu, H. L.; Tam, K. C. *Can. J. Chem. Eng.* **2011**, *89*, 1.
24. Turbak, A. F.; Snyder, F. W.; Sandberg, K. R. *J. Appl. Polym. Sci.* **1983**, *28*, 815.
25. Ahola, S.; Österberg, M.; Laine, J. *Cellulose* **2008**, *15*, 303.
26. Zimmermann, T.; Bordeanu, N.; Strub, E. *Carbohydr. Polym.* **2010**, *79*, 1086.
27. Eriksen, Ø.; Syverud, K.; Gregersen, Ø. W. *Nord. Pulp Pap. Res. J.* **2008**, *23*, 299.
28. Isogai, A.; Saito, T.; Fukuzumi, H. *Nanoscale* **2011**, *3*, 71.
29. Saito, T.; Isogai, A. *Biomarcromoleculars* **2005**, *5*, 1983.
30. Xu, Q. H.; Gao, Y.; Qin, M. H.; Wu, K. L.; Fu, Y. J.; Zhao, J. *Int. J. Biol. Macromol.* **2013**, *60*, 241.
31. Garvey, C. J.; Parker, I. H.; Simon, G. P. *Macromol. Chem. Phys.* **2005**, *206*, 1568.
32. Fukuzumi, H.; Saito, T.; Isogai, A. *Carbohydr. Polym.* **2013**, *93*, 172.
33. Zhang, X. Y.; Liu, W. X. *Bioresources* **2010**, *5*, 1895.
34. Habibi, Y.; Chanzy, H.; Vignon, M. R. *Cellulose* **2006**, *13*, 679.
35. Praskalo, J.; Kostic, M.; Potthast, A.; Popov, G.; Pejic, B.; Skundric, P. *Carbohydr. Polym.* **2009**, *77*, 791.
36. Saito, T.; Nishiyama, Y.; Putaux, J.-L.; Vignon, M.; Isogai, A. *Biomacromolecules* **2006**, *7*, 1687.
37. Besbes, I.; Alila, S.; Boufi, S. *Carbohydr. Polym.* **2011**, *84*, 975.
38. Fukuzumi, H. Available at: http://repository.dl.itc.U-tokyo.ac.Jp/dspace/bitstream/2261/52027/1/39–097097.pdf.
39. Klemm, D.; Heublein, B.; Fink, H. P.; Bohn, A. *Angew. Chem. Int. Edit.* **2005**, *44*, 3358.
40. Jean, B.; Dubreuil, F.; Heux, L.; Cousin, F. *Langmuir* **2008**, *24*, 3452.
41. Liu, W.; Ni, Y.; Xiao, H. *J. Pulp Pap Sci.* **2003**, *29*, 145.
42. Hedborg, F.; Lindstrom, T. *Nord. Pulp Pap. Res. J.* **1996**, *11*, 254.